

IRRE EMILIA ROMAGNA

Gruppo di ricerca sulla storia mondiale

DOSSIER

Materiali di studio

INDICE

1. Peter B. deMenocal

Cultural Responses to Climate Change During the Late Holocene

in www.sciencemag.org SCIENCE VOL 292 27 APRIL 2001 (pag.667-673)

2. Due pagine che presentano la struttura di

Terra.sat. Dizionario enciclopedico geografico, edizione realizzata per *il Corriere della Sera*, 2000 (prima pubblicazione in Gran Bretagna nel 1994 da Dorling Kindersley Limited, London), che dedica a ciascuna nazione del Mondo una scheda più o meno ampia che comprende sia testi sia numerosi grafici e tabelle.

54. Interannual cross-correlations are ~ 0.5 back to 1750 and ~ 0.25 back to 1500.
55. R. S. Bradley, P. D. Jones, *Holocene* **3**, 367 (1993).
56. J. M. Grove, *The Little Ice Age* (Methuen, New York, 1988).
57. M. K. Hughes, H. F. Diaz, *Clim. Change* **26**, 109 (1994).
58. World Data Center for Paleoclimatology (www.ngdc.noaa.gov/paleo/data.html).
59. W. T. Bell, A. E. J. Ogilvie, *Clim. Change* **1**, 331 (1978).
60. M. J. Ingram, D. J. Underhill, G. Farmer, in *Climate and History: Studies in Past Climates and Their Impact on Man*, T. M. L. Wigley, M. J. Ingram, G. Farmer, Eds. (Cambridge Univ. Press, Cambridge, 1981), pp. 180–213.
61. A. E. J. Ogilvie, T. Jónsson, *Clim. Change* **48**, 9 (2001).
62. H. H. Lamb, *Climate, Present, Past and Future* (Methuen, London, 1977), vol. 2.
63. G. Manley, *Q. J. R. Meteorol. Soc.* **100**, 389 (1974).
64. E. R. Cook, *Clim. Dyn.* **11**, 211 (1995).
65. J. M. Lough, D. J. Barnes, *J. Exp. Mar. Biol. Ecol.* **211**, 29 (1997).
66. K. R. Briffa, T. J. Osborn, *Science* **284**, 926 (1999).
67. P. D. Jones, *J. Clim.* **3**, 1193 (1990).
68. F. E. Urban, J. E. Cole, J. T. Overpeck, *Nature* **407**, 989 (2000).
69. V. Morgan, T. D. van Ommen, *Holocene* **7**, 351 (1997).
70. L. G. Thompson, E. Mosley-Thompson, B. M. Arno, *Science* **234**, 631 (1984).
71. The authors were supported by the UK Natural Environment Research Council (GR3/12107) and by the U.S. Department of Energy (DE-FG02-98ER62601). Additional support came from NOAA's Office of Global Programs and the DOE's Office of Energy Research in conjunction with the Climate Change Data and Detection element. The authors thank their many paleoclimatic colleagues for making their data available. Particular thanks also go to T. Barnett, R. Bradley, E. Cook, T. Crowley, M. Hughes, J. Luterbacher, M. Mann, and F. Schweingruber for countless discussions over the last 10 years or more.

REVIEW

Cultural Responses to Climate Change During the Late Holocene

Peter B. deMenocal

Modern complex societies exhibit marked resilience to interannual-to-decadal droughts, but cultural responses to multidecadal-to-multicentury droughts can only be addressed by integrating detailed archaeological and paleoclimatic records. Four case studies drawn from New and Old World civilizations document societal responses to prolonged drought, including population dislocations, urban abandonment, and state collapse. Further study of past cultural adaptations to persistent climate change may provide valuable perspective on possible responses of modern societies to future climate change.

In the spring of 1785, the geologist James Hutton presented a lecture to the Royal Society of Edinburgh that changed scientific inquiry into natural processes. The essence of his view was simple enough: The present is the key to understanding the past. Hutton recognized that slow geologic processes such as erosion or uplift could produce sedimentary strata or mountain ranges. In 1795, he wrote that “we find no vestige of a beginning—no prospect of an end. . . . Not only are no powers to be employed that are not natural to the globe, no actions to be admitted of except those of which we know the principle and no extraordinary events to be alleged in order to explain a common experience . . .” (1). This view was not accepted by most natural scientists at the time because it required full acceptance of the expanse of geologic time and rejection of the prevalent views of a young Earth. Future generations of scientists, however, most notably Charles Darwin half a century later, were encouraged by this new way of thinking to interpret their observations on the basis of what they knew of modern processes.

To understand how and why climates change, we have to invoke a corollary to Hutton's view: The past must be used to understand the present. Modern instrumental

records are sufficiently long to document climate phenomena that vary at interannual time scales, such as El Niño, but they are too short to resolve multidecadal- to century-scale climate variability that we know to exist from detailed tree-ring, coral, and lake sediment records spanning the past 500 to 1000 years (2, 3). Similarly, the socioeconomic impacts of recent El Niño/La Niña events are well documented (4), but little is known about the societal impacts of longer period climatic excursions. Without knowing the full range of climatic variability at time scales of a few decades to a few millennia, it is difficult to place our understanding of modern climate variability, and its socioeconomic impacts, within the context of how Earth climate actually behaves, both naturally and as a result of anthropogenic increases of greenhouse gasses (3).

Historic and Prehistoric Drought in North America

Excellent examples of the value of past climate records can be gleaned from the history of drought in the United States. Water availability, rather than temperature, is the key climatic determinant for life in semiarid expanses across the planet. Drought often conjures up images of the Dust Bowl drought of the 1930s, which lasted ~ 6 years (1933–38) and resulted in one of the most devastating and well-documented agricultural, economic, and social disasters in the history of the Unit-

ed States. The drought was triggered by a large and widespread reduction in rainfall across the American West, particularly across the northern Great Plains (5). It displaced millions of people, cost over \$1 billion (in 1930s U.S. dollars) in federal support, and contributed to a nascent economic collapse. Subsequent analysis of the Dust Bowl drought has revealed that its tremendous socioeconomic impact was, in part, due to wanton agricultural practices and overcapitalization just before the drought, when rainfall had been more abundant (5). A subsequent decadal-scale drought in the 1950s (Fig. 1, A and B) was also severe but less widespread, mainly impacting the American Southwest, where improved land use practices and disaster relief programs mitigated its effects.

How did the 1930s and 1950s droughts compare with other historic and prehistoric droughts? In a comprehensive analysis of hundreds of tree-ring chronologies from across the United States, Cook and others established a network of summer drought reconstructions extending back to 1200 A.D. (6, 7) (Fig. 1A). This reconstruction documents much more persistent droughts before the 1600s (7). These so-called “megadroughts” were extremely intense, persisted over many decades, and recurred across the American Southwest roughly once or twice every 500 years (Fig. 1, A through D). Reconstructed conditions during the largest of these multidecadal droughts far surpassed those during droughts recorded within the past ~ 150 years (the period for which extensive instrumental data are available). Evidence for these and other megadroughts has been found in detailed lake sediment records (8), with additional evidence for even longer, century-scale droughts in California before 1350 and 1110 A.D. (9).

The most severe drought in the southwestern United States within the past 800 years

Lamont-Doherty Earth Observatory of Columbia University, Palisades, NY 10964, USA. E-mail: peter@ldeo.columbia.edu

spanned an ~ 22 -year period between 1572 and 1593 A.D. (7) (Fig. 1C). The reconstructed spatial drought pattern at the peak of this dry period in 1583 A.D. shows extreme drought conditions extending across the American Southwest (Fig. 1C). Dry conditions apparently extended eastward and persisted into the early 1600s as far east as coastal Virginia (10). On the basis of a 700-year tree-ring chronology from northeastern Virginia, Stahle *et al.* conclude that the intervals spanning 1587 to 1589 A.D. and 1606 to 1612 A.D. were the driest periods in the past 700 years (10). In August of 1587 A.D., the first English colonists arrived and settled in Roanoke, Virginia. This small group of settlers became known subsequently as the Lost Colony, because the entire Roanoke settlement had vanished by the time the English resupply ships returned 4 years later. Originally attributed to poor planning and inadequate supplies, the failure of the Roanoke settlement is now understood within the context of this severe drought, which began, to their monumental bad luck, just when the settlers arrived (10). A larger colonial settlement was established subsequently in James-

town, Virginia, in April of 1607 A.D., and the settlers also suffered greatly. Within 25 years, over 80% of the population died, mainly of malnutrition (10).

Although appreciably less severe than the drought of the 1580s, the 26-year "Great Drought" of the 1280s (11) was similarly prolonged and widespread (Fig. 1D). By the time of this drought, the Anasazi, ancestors of modern Pueblo Indians, had long established elegant stone and adobe villages in the semi-arid highlands and canyons of the American Southwest. Archaeological investigations of Anasazi settlements have documented that many sites were abandoned abruptly near the end of the 13th century A.D. Cited reasons for the collapse of the Anasazi include emergent balkanization, warfare, and religious turmoil within the region, as well as the onset of severe drought conditions and regional deforestation (11, 12). Whether the multidecadal drought of the 1280s was the determining factor in the collapse of the Anasazi continues to be debated (13, 14), but current archaeological evidence firmly implicates drought as a contributing destabilizing factor (12, 14).

Modes and Mechanisms of Holocene Climate Variability

The relatively recent droughts described above persisted from a few years to a few decades. Complex societies can, and do, adapt readily to interannual-to-decadal fluctuations in water availability, but more persistent droughts present a different set of challenges and coping strategies. Multidecadal- to multicentury-scale droughts are now known to have punctuated the warm climate of the Holocene epoch [the past 11,700 calendar years before the present (calendar yr B.P.)]. Furthermore, transitions into and out of these climate shifts can be very abrupt, occurring in less than a decade (15). The Holocene was once thought to have been climatically stable (16), but detailed and well-dated paleoclimate records now show that Holocene climate was punctuated by several widespread cooling events, which persisted for many centuries and recurred roughly every 1500 ± 500 years (17–22) (Fig. 2).

Paleoceanographic data indicate that these events were associated with changes in sub-polar (19) and subtropical (21, 22) surface ocean circulation (Fig. 2), as well as marked changes in terrestrial climates (17, 18, 23, 24). These events appear to have occurred synchronously across the North Atlantic (21), with possible antiphase behavior in the northwest Atlantic (25). Deep-sea sediment evidence for deep-ocean circulation changes associated with these Holocene events is, at present, equivocal (19, 26), although other supportive evidence has been presented (20, 27, 28). The millennial-scale pacing of Holocene climate variability implicates mechanisms with long time constants, such as thermohaline circulation or ocean-atmosphere coupling (26, 29), which govern modern climate stability.

Analysis of the most recent millennial-scale Holocene climate cycle, the Little Ice Age [circa (ca.) 1300 to 1870 A.D.] and the preceding Medieval Warm Period (ca. 800 to 1300 A.D.), suggests that the primary factors affecting global temperature variability over the past millennium were variations in solar irradiance and volcanism, which together account for 40 to 60% of the reconstructed temperature variability (30). Climate models require an additional forcing agent, the anthropogenic rise in greenhouse gases, to account for 20th-century warmth (30, 31). Strong correlations of solar irradiance variability (32, 33) with surface temperature (30, 31) and regional drought (34, 35) over the past millennium implicate solar variability as an important factor influencing global climate over multidecadal-to-multicentury time scales. However, the role of solar variability in forcing the full suite of millennial-scale climate variations during the Holocene (and the last glacial) is complicated by the absence

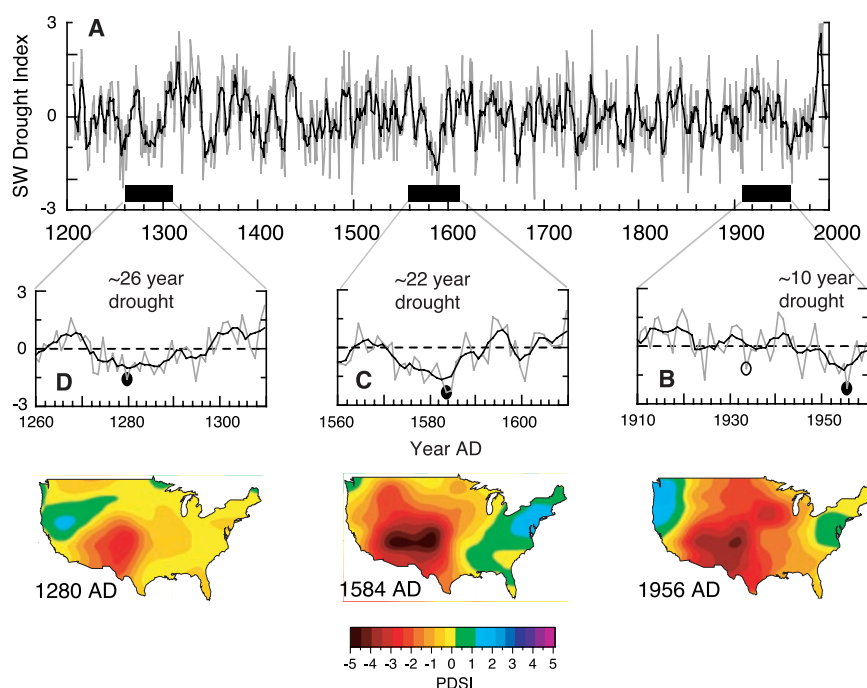


Fig. 1. Drought history [1200 to 1994 A.D. (6, 7)] for the American Southwest, reconstructed by using a spatial network of tree-ring chronologies across the United States (black curves show the decadal average; gray curves represent the full annual-resolution record). (A) This time series is the first varimax-rotated empirical orthogonal function factor from these records and reflects the drought history for the American Southwest over a region roughly including Arizona, Utah, Nevada, Colorado, New Mexico, and west Texas (6, 7). Reconstructed spatial drought index [the Palmer Drought Severity Index (PDSI)] patterns are shown for (B) the ~ 6 -year Dust Bowl drought of the 1930s, which was largely restricted to the northern and western Great Plains [peak drought was in 1934 (open circle)], and the widespread ~ 10 -year drought of the 1950s [peak drought was in 1956 (solid circle)]; (C) the ~ 22 -year Southwest drought of the 1580s [peak drought was in 1583 (solid circle)]; and (D) the ~ 26 -year Southwest drought of the 1280s [peak drought was in 1280 (solid circle)]. Relatively short (multiyear) but intense droughts such as the 1930s Dust Bowl period (B) were found to recur roughly once or twice per century (6), whereas multidecadal droughts occur only a few times in a millennium.

of 1500 ± 500 year variability in the atmospheric ^{14}C record (36) and its generally inconsistent match with Holocene climate anomalies (Fig. 2). The ^{14}C record does exhibit substantial variance at periods near 2200 to 2500 years [the Hallstadzeit cycle (36)].

Cultural Responses to Late Holocene Climate Variations

How did past cultures respond to the longer, multicentury-scale climate changes that punctuated late Holocene climate? Placing the archaeological record of cultural change within the context of detailed and well-dated Holocene paleoclimate records presents opportunities to examine how large, complex societies responded to long-term, persistent changes in climate. At some times during the late Holocene, whole empires collapsed and their people were diminished to much lower subsistence levels, whereas in other cases, populations migrated and adapted to new subsistence modes. In all cases, the observed societal response reflects an interaction between human cultural elements (socioeconomic, political, and secular stresses) and persistent multicentury shifts in climate. Four case studies drawn from the joint archaeological and paleoclimate histories of the New and Old World illustrate past cultural responses to late Holocene climate change: the collapse of the Akkadian (ca. 4200 calendar yr B.P.), Classic Maya (ca. 1200 calendar yr B.P.), Mochica (ca. 1500 calendar yr B.P.), and Tiwanaku (ca. 1000 calendar yr B.P.) empires.

Akkadian collapse (Mesopotamia, ca. 4200 calendar yr B.P.). Under the rule of Sargon of Akkad, the first empire was established between ca. 4300 and 4200 calendar yr B.P. on the broad, flat alluvial plain between the Tigris and Euphrates Rivers (37). Akkadian imperialization of the region linked the productive but remote rain-fed agricultural lands of northern Mesopotamia with the irrigation agriculture tracts of southern Mesopotamian cities. After ~100 years of prosperity, however, the Akkadian empire collapsed abruptly at ca. 4170 ± 150 calendar yr B.P. (37, 38). Archaeological evidence documents widespread abandonment of the agricultural plains of northern Mesopotamia (37) and dramatic influxes of refugees into southern Mesopotamia, where populations swelled (37, 39) (Fig. 3). A 180-km-long wall, the “Repeller of the Amorites,” was built across central Mesopotamia to stem nomadic incursions to the south. Resettlement of the northern plains by smaller, sedentary populations occurred near 3900 calendar yr B.P., ~300 years after the collapse (37). The stratigraphic level representing the collapse at Tell Leilan, northeast Syria, is overlain by a thick (~100 cm) accumulation of wind-blown silts, which was devoid of artifacts (37), sug-

gesting a sudden shift to more arid conditions. Social collapse evidently occurred despite archaeological evidence that the Akkadians had implemented grain storage and water regulation technologies to buffer themselves against the large interannual variations in rainfall that characterize this region (37).

Using a deep-sea sediment core from the Gulf of Oman, Cullen *et al.* (40) reconstructed a detailed record of Holocene variations in regional dust export based on mineralogical

and geochemical tracers of wind-borne sediments from Mesopotamian sources (Fig. 4). Closely dated by a sequence of calibrated radiocarbon dates, the Gulf of Oman core documents a dramatic ~300-year increase in eolian dolomite and carbonate, which commenced at 4025 ± 125 calendar yr B.P. Isotopic ($^{87}\text{Sr}/^{86}\text{Sr}$) analyses demonstrate that the increased eolian dust was derived from Mesopotamian sources (40) (Fig. 4). Geochemical similarity of volcanic tephra shards found at Tell Leilan and in the deep-sea

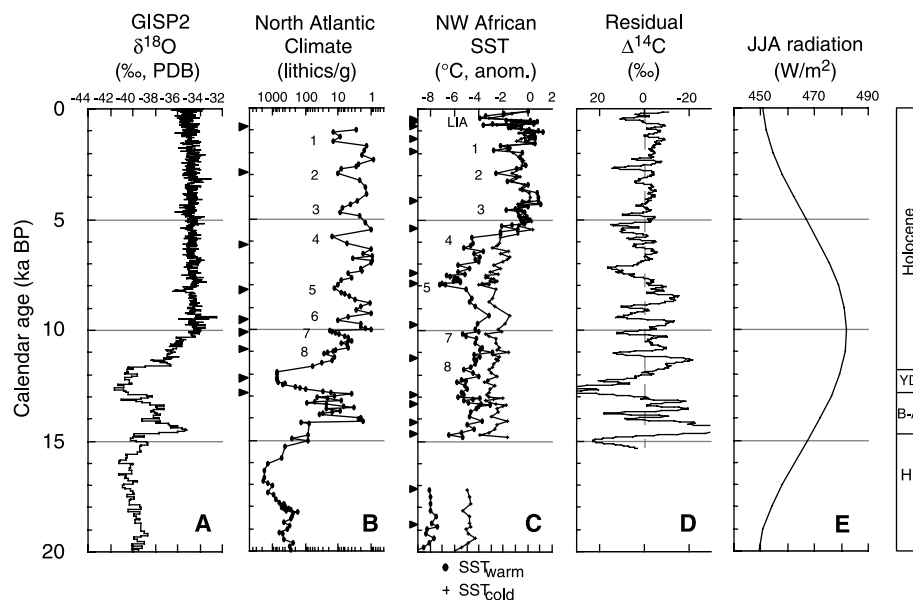


Fig. 2. Millennial-scale climate variability during the Holocene. (A) Oxygen isotope data from the Greenland Ice Sheet Project 2 (GISP2) ice core initially suggested that Holocene climates were stable (16) [‰, per mil; PDB, Pee Dee belemnite]; however, detailed and well-dated Holocene records of (B) subpolar and (C) subtropical North Atlantic sea surface temperatures (SSTs) (19, 21) document synchronous cooling events recurring at 1500 ± 500 year intervals throughout the Holocene (and Late Pleistocene) (anom., temperature anomalies; LIA, Little Ice Age). Solid triangles indicate calibrated calendar ages of radiocarbon dates on monospecific planktonic foraminifera. Analysis of global surface temperature records has suggested that solar irradiance variability accounts for much of the observed temperature variability over the past millennium (30, 31), although variations in solar irradiance spanning the entire Holocene [as partially represented by (D) the production-corrected atmospheric ^{14}C record (32, 33, 36)] do not match the paleoclimate records. (E) Boreal summer [June, July, August (JJA)] solar insolation at 20°N . Ages for the Heinrich Layer 1 (H1) and Younger Dryas (YD) cold periods and the Bølling-Allerød (B-A) and Holocene warm periods are shown to the right [ka, thousand years ago].



Fig. 3. Excavated sample of residential occupation (600 m^2) within the lower town of Tell Leilan, northeast Syria (100 ha), during the terminal Akkadian empire occupation. Abrupt climate change (ca. 2200 B.C.) forced the Akkadian abandonment of rain-fed agriculture plains of northern Mesopotamia. [Photo credit: H. Weiss/Yale University]

sediment core provided further evidence that the Akkadian collapse and climate change events were synchronous (40). Enhanced regional aridity is also indicated by increased eolian quartz deposition in nearby Lake Van at the headwaters of the Tigris River (41) and by paleoclimate records from the Levant (42). The combined archaeological and paleoclimate evidence strongly implicates abrupt climate change as a key factor leading to the demise of this highly complex society.

The onset of sudden aridification in Mesopotamia near 4100 calendar yr B.P. coincided with a widespread cooling in the North Atlantic (19, 21). During this event, termed Holocene Event 3 (Fig. 2), Atlantic subpolar and subtropical surface waters cooled by 1° to 2°C (19, 21). The headwaters of the Tigris and Euphrates Rivers are fed by elevation-induced capture of winter Mediterranean rainfall. Analysis of the modern instrumental record shows that large (50%) interannual reductions in Mesopotamian water supply result when subpolar northwest Atlantic sea surface temperatures are anomalously cool (43). The aridification of Mesopotamia near 4100 calendar yr B.P. may thus have been

related to the onset of cooler sea surface temperatures in the North Atlantic.

Classic Maya collapse (Yucatán Peninsula, ca. 1200 calendar yr B.P.). The Preclassic Maya culture occupied vast lowland and highland regions of Mesoamerica from the second millennium B.C. to ca. 250 A.D. The onset of the Early Classic period after 250 A.D. marks the rapid growth of a more complex, stratified, and intellectually and artistically prolific empire. The hallmark accomplishments of Early (250 to 550 A.D.) and especially Late (550 to 850 A.D.) Classic Maya cultures include the development of trade networks spanning Mesoamerica, expansive urban centers, the erection of monumental stelae, and advances in astronomy and mathematics (44).

The Classic Maya empire collapsed at the peak of their cultural development between ca. 750 and 900 A.D., as determined by the number of sites engaged in monument construction across Mesoamerica at any given time (45) (Fig. 5). Following the apex of monument construction in 721 A.D., signs of collapse began to show between 750 and 790 A.D. Construction effectively ceased

throughout the region after 830 A.D., and in 909 A.D., the last monument in southern Quintana Roo, Mexico, was inscribed with the Maya Long Count date (44). Many reasons for the collapse have been cited, including overpopulation, deforestation and soil erosion, social upheaval, warfare, and disease, as well as natural phenomena, such as climate change (46, 47). Deforestation, erosion, and dense human occupation are well-documented in many regions before the collapse (46, 48, 49).

The first unambiguous evidence for the role of climate change in the collapse of the Classic Maya (50) came from lake sediments, which documented an abrupt shift to more arid conditions in the central Yucatán Peninsula (Mexico) between 1300 to 1100 calendar yr B.P. (800 to 1000 A.D.) (Fig. 6). Sediment composition and stable isotopic analyses of ostracode shells preserved in sediment cores from the closed-basin Lakes Chichancanab (50) and Punta Laguna (51) in the central Yucatán indicate that the region was subjected to an ~200-year period of persistently arid and highly evaporative conditions centered near 1200 calendar yr B.P. (900 A.D.) (Fig. 6).

The densely populated southern lowlands of the Yucatán Peninsula were highly reliant on surface water supplies for human and agricultural needs, and it was these regions that were most acutely affected during the drought from 800 to 1000 A.D. Archaeological excavations estimate that lowland population densities decreased from ~200 persons/km² at the peak of the Late Classic period to less than 100 persons/km² by ca. 900 A.D.; by 1500 A.D., many watersheds had been completely abandoned (48). An additional dry period predating the collapse was noted at 580 A.D. in the higher resolution core record from Lake Punta Laguna (51) (Fig. 6). This century-scale dry period coincides with the Maya Hiatus at the Early/Late Classic Maya boundary, when monument construction was briefly curtailed (from ca. 530 to 650 A.D.) (44, 45, 48).

Moche IV–V Transformation (coastal Peru, ca. 1500 calendar yr B.P.). Pre-Columbian coastal and highland Peruvian civilizations offer exceptional insight into past linkages between culture and climate change because they sustained densely populated, complex, agrarian cultures in very challenging environments. The Peruvian coast is extremely arid and requires a high reliance on irrigation to support agriculture, yet these regions sustained large populations for many centuries.

Known for their sophisticated metallurgy and monumental adobe brick structures, the Mochica polity established urban centers and controlled the entire northern Peruvian coastline south of the Sechura desert from ca. 300 to 500 A.D. (early Moche IV period) (52). One such locality, the capital site of Moche,

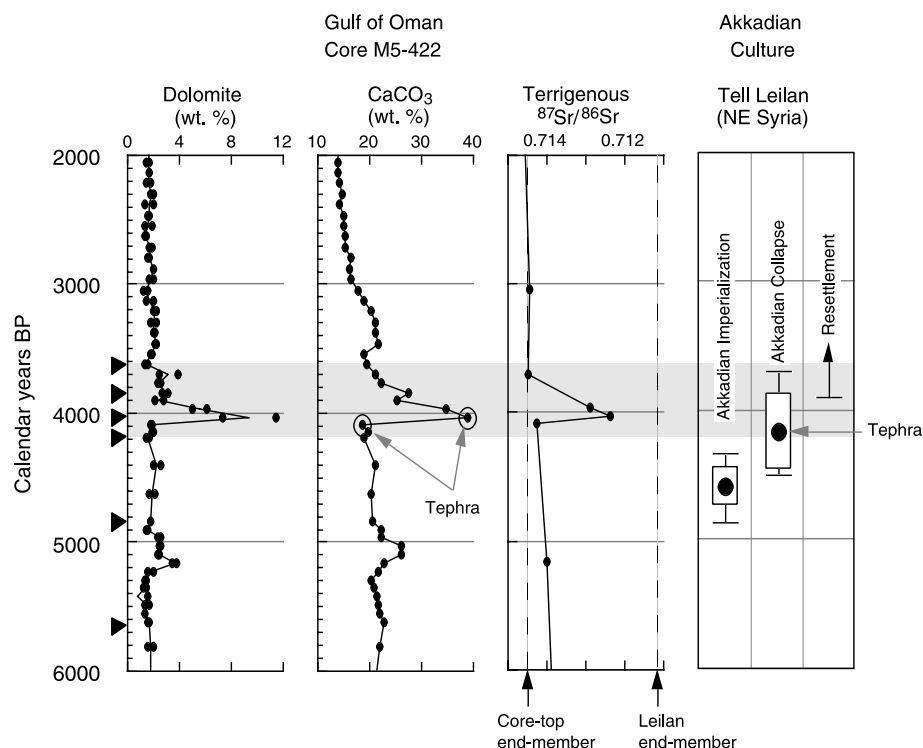


Fig. 4. Mesopotamian paleoclimate and the collapse of the Akkadian empire. Detailed radiocarbon dates of archaeological remains at Tell Leilan, northeast Syria, document the abandonment and incipient collapse of the Akkadian empire near 4170 ± 150 calendar yr B.P. (37). A late Holocene record (40) of Mesopotamian aridity was reconstructed by quantifying wind-borne sediment components in a deep-sea sediment core from the Gulf of Oman, which is directly downwind of eolian dust source areas in Iraq, Kuwait, and Syria. The severalfold increase in eolian dolomite and calcite commencing at 4025 ± 125 calendar yr B.P. reflects an ~300-year interval of increased Mesopotamian aridity. A Mesopotamian provenance for this dust peak is indicated from detrital (mineral) fraction Sr (and Nd) isotopic analyses, which show a marked shift toward the measured Mesopotamian (Tell Leilan abandonment) composition (40). Solid triangles indicate calibrated calendar ages of radiocarbon dates on monospecific planktonic foraminifera.

boasts the largest adobe structure in the New World, the Huaca del Sol (52). This immense coastal site and the cities it served were very abruptly abandoned near 600 A.D. Archaeological evidence shows that main irrigation channels had been overrun by sand dunes at the time of abandonment. The subsequent Moche V culture was reestablished farther inland, near the confluence of highland rivers draining the Andean foothills, where runoff was more dependable, between 600 and 750 A.D. The Moche IV–V Transformation was unprecedented in scope, scale, and rapidity for this region (52).

An annual resolution record of regional precipitation changes from the Quelccaya ice core (Peru) firmly implicates climate change as a leading factor underlying the Moche IV–V Transformation (52). Variations in oxygen isotopes, accumulation rate, and insoluble particle concentration in this ice core document large changes in regional climate spanning the past 1500 years, which can be used to place the cultural records within their paleoclimatic contexts (52, 53). Comparison of the paleoclimatic and cultural histories indicates that the Moche IV–V Transformation near 600 A.D. was immediately preceded by an ~30-year period of reduced regional precipitation (lower ice accumulation between 563 and 594 A.D.) and corresponded with an ~60-year interval of increased wind-borne particles in the ice (Fig. 7). The loss of Moche IV coastal irrigation channels to encroaching sand dunes and the population migration to the better watered highland valleys are consistent responses to the enhanced regional aridity indicated by the ice core (52). Paulsen (54) recognized several coastal to highland population shifts throughout the first and second millennium A.D. (Fig. 7), noting a general seesaw relation between the rise and fall of coastal and highland agrarian cultures in both Peru and Ecuador. As discussed by Thompson *et al.* (53), these ancient coastal to highland population shifts closely corresponded with the largest ice accumulation (precipitation) changes recorded in the Quelccaya ice core record (Fig. 7). Of particular paleoclimatic interest is the evidently synchronous onset of arid conditions in the tropics of both hemispheres (Peru and the Yucatán) near 900 and 600 A.D. (51) (Figs. 6 and 7).

Tiwanaku collapse (Bolivian-Peruvian altiplano, ca. 1000 calendar yr B.P.). The Tiwanaku culture thrived for nearly 1500 years (300 B.C. to 1100 A.D.) in urban and rural agrarian settings surrounding Lake Titicaca in the southern Bolivian-Peruvian altiplano (~4000-m elevation) (55, 56). Through the ingenious use of raised field cultivation, which promotes efficient nutrient recycling and uses irrigation canals to thermally buffer crops against killing frosts, the Tiwanaku



Fig. 5. Structures emerge from the surrounding tropical forest at the Maya archaeological site of Tikal in Petén, Guatemala. At its peak in the Late Classic period (ca. 800 A.D.), this urban center in the southern Maya lowlands supported ~60,000 inhabitants. It was largely depopulated after the ninth-century A.D. demographic collapse. [Photo credit: M. Brenner]

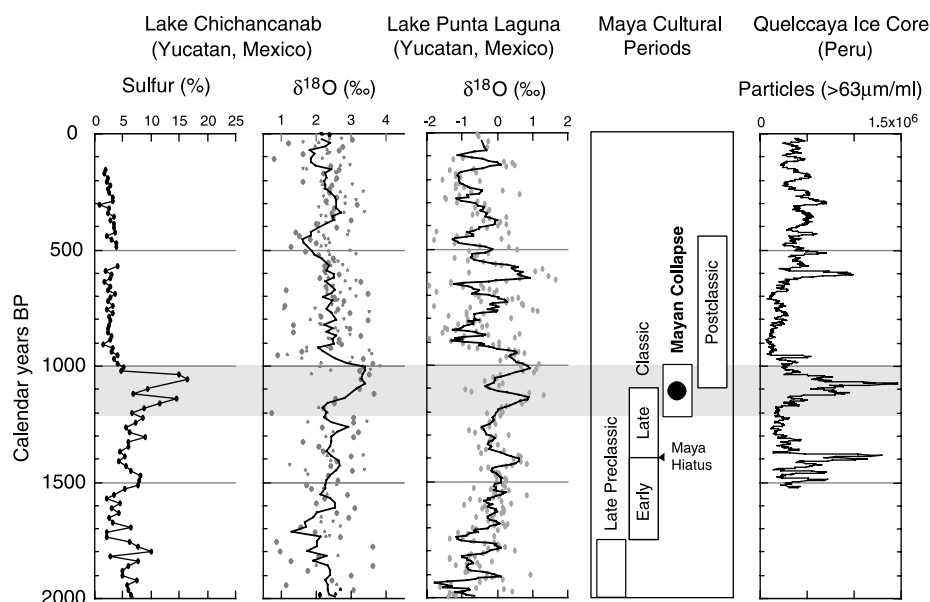


Fig. 6. Mesoamerican paleoclimate and the Classic Maya collapse. Incipient collapse of the Classic Maya civilization began near 750 to 790 A.D., and the last Maya stela or monument construction has been dated at 909 A.D. on the basis of Maya Long Count inscriptions (44, 45). Well-dated sediment cores from Lakes Chichancanab (50) and Punta Laguna (51) (northern Yucatán Peninsula, Mexico) document an abrupt onset of more arid conditions spanning ~200 years between 800 and 1000 A.D., as evidenced by more evaporative (higher) $\delta^{18}\text{O}$ values and increases in gypsum precipitation (elevated sulfur content) (highlighted by gray bar through all panels). A century-long dry period coincides with the Maya Hiatus centered near 580 A.D., which documents a period (530 to 650 A.D.) of marked curtailed monument construction (44, 45, 48). Wind-borne particle concentrations from the annually dated Quelccaya ice core in the Peruvian altiplano are also shown (53).

were able to sustain an urban complex with an estimated population of nearly half a million people (55). The massive urban center at Lake Titicaca served as the capital of an expanding state society that eventually exploited regions extending to the Peruvian coastal desert and foothills.

The densely settled Tiwanaku urban centers and raised fields were abandoned abruptly near 1100 A.D. (55, 56). Full collapse of the Tiwanaku state occurred over the 12th to 15th centuries. The Quelccaya ice core was drilled just 200 km northwest of Lake Titicaca (53) and thus provides valuable insight into the paleoclimatic contexts of the Tiwanaku abandonment and collapse. Comparison of the Tiwanaku cultural changes with the Quelccaya isotopic and ice accumulation records shows a close coincidence between the abandonment and the onset of increasingly arid conditions (lower ice accumulation rate) (Fig. 7). Conditions markedly drier than those of today persisted for several centuries, commencing after 1040 A.D. (53). Sediment cores from Lake Titicaca document an ~10-m drop in lake level at this time (56). It has been proposed that the sudden onset and

multicentury persistence of more arid conditions would have dramatically impacted the productivity of the raised field agriculture system and, consequently, its ability to sustain swelling Tiwanaku urban and rural populations (53, 55, 56).

Past Cultural Responses to Climate Change

What can be learned from these ancient cultural responses to prolonged drought? The climatic perturbations associated with these late Holocene societal dislocations were extreme in their duration and intensity, far surpassing droughts recorded during the modern instrumental period. As shown in Fig. 1A, interannual droughts occur many times within a given generation, and decadal droughts recur infrequently across many generations. Multidecadal to multicentury scale droughts are much rarer but are nonetheless integral components of natural climate variability. Well-dated and detailed paleoclimate records from climatically sensitive locations bear witness to the occurrence and severity of these multidecadal-to-multicentury droughts (Figs. 2, 4, and 6).

For the examples discussed above, available paleoclimate and archaeological data show that societal collapse and prolonged drought were coincident within respective dating uncertainties. Coincidence alone cannot demonstrate causality; indeed, each of these cultural collapses had been at one time interpreted solely in terms of human factors unrelated to natural climate variability, such as warfare, overpopulation, deforestation, and resource depletion. However, joint interpretation of the paleoclimatic and archaeological evidence now underscores the important role of persistent, long-term drought in the collapse of the Akkadian (37, 39, 40), Maya (46–48, 50), Mochica (52, 53), and Tiwanaku (53, 55, 56) civilizations. These examples show that, challenged by unprecedented environmental stresses, cultures can shift to lower subsistence levels by reducing social complexity, abandoning urban centers, and reorganizing systems of supply and production (39).

Recalling James Hutton's uniformitarian premise, what makes these ancient events so relevant to modern times is that they simultaneously document both the resilience and vulnerability of large, complex civilizations to environmental variability. Complex societies are neither powerless pawns nor infinitely adaptive to climate variability. As with modern cultures, the ancients adapted to and thrived in marginal environments with large interannual climate variability. As with ancient cultures, modern civilizations (regrettably) gauge their ability to adapt to future climate variations on the basis of what is known from historical (oral or instrumental) records. What differentiates these ancient cultures from our own is that they alone have witnessed the onset and persistence of unprecedented drought that continued for many decades to centuries. Efforts to understand past cultural responses to large and persistent climate changes may prove instructive for assessing modern societal preparedness for a changing and uncertain future (57).

References and Notes

1. J. Hutton, *Theory of the Earth*, with proofs and illustrations (Creech, Edinburgh, 1795).
2. J. T. Overpeck, *Science* **271**, 1820 (1996).
3. _____, R. Webb, *Proc. Natl. Acad. Sci. U.S.A.* **97**, 1335 (2000).
4. M. Cane, G. Eshel, R. W. Buckland, *Nature* **370**, 204 (1994).
5. R. A. Warrick, in *Drought in the Great Plains: A Case Study of Research on Climate and Society in the USA*, J. Ausubel, A. K. Biswas, Eds., *NASA Proceedings Series: Climate Constraints and Human Activities* (Perigamon, New York, 1980).
6. E. R. Cook, D. M. Meko, D. W. Stahle, M. K. Cleaveland, *J. Clim.* **12**, 1145 (1999).
7. E. A. Cook, Southwestern USA Drought Index Reconstruction, International Tree-Ring Data Bank, IGBP PAGES/World Data Center for Paleoclimatology, Data Contribution Series #2000-053 (NOAA/NGDC Paleoclimatology Program, Boulder, CO, 2000).
8. C. Woodhouse, J. T. Overpeck, *Bull. Am. Meteorol. Soc.* **72**, 2693 (1998).

Quelccaya Ice Core (Peru)

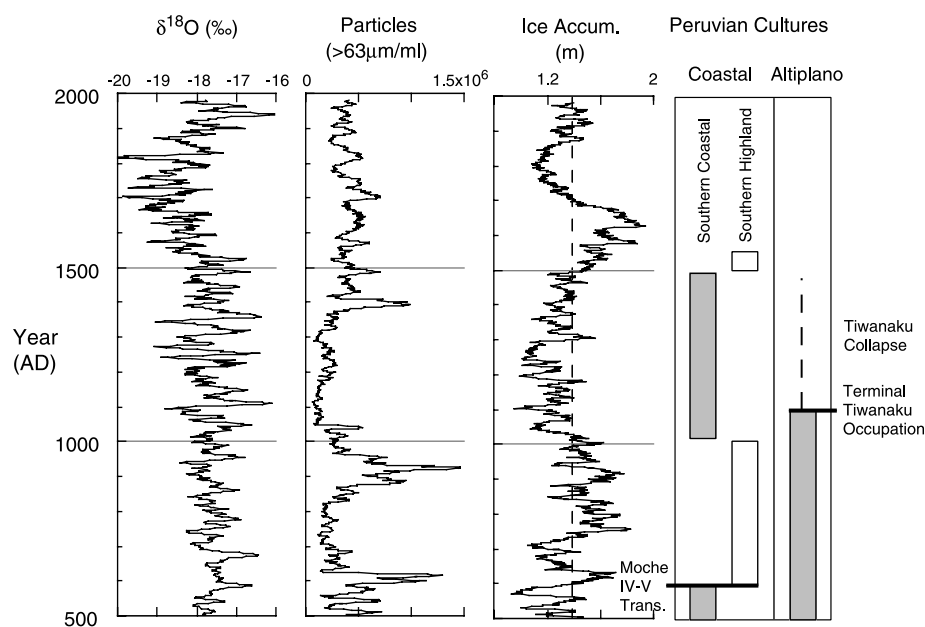


Fig. 7. Peruvian coastal, highland, and altiplano paleoclimate and the Moche IV–V Transformation and Tiwanaku collapse. The Mochica civilization imperialized the desert coast of Peru between 300 and 500 A.D. (Moche IV period) but then abruptly abandoned coastal urban centers and moved to better watered highland valleys between 600 and 750 A.D. (Moche V period) (52). The Moche IV–V Transformation was evidently just one of a series of oscillatory population migrations between the arid coast and the more humid highlands (54). The annually dated Quelccaya ice core in southern Peru documents large changes in regional climate spanning the past 1500 years (53), notably multicentury shifts in precipitation that coincide with the coastal to highland settlement dislocations. On the shores of Lake Titicaca in the Bolivian-Peruvian altiplano, the Tiwanaku civilization established large urban centers and populations between 300 B.C. and 1100 A.D. Tiwanaku urban centers and cultivation fields were abruptly abandoned after 1100 A.D., and the Tiwanaku culture had completely collapsed by ca. 1400 A.D. (55, 56). The Tiwanaku abandonment and collapse coincide with a multicentury interval of reduced precipitation, as determined by the ice accumulation record at Quelccaya, ~200 km northwest of Lake Titicaca (56).

9. S. Stine, *Nature* **369**, 546 (1994).
10. D. W. Stahle, M. K. Cleaveland, D. B. Blanton, M. D. Therrell, D. A. Gay, *Science* **280**, 564 (1998).
11. A. E. Douglass, *Natl. Geogr.* **54**, 737 (1929).
12. L. S. Cordell, *Archaeology of the Southwest* (Academic Press, San Diego, CA, 1997).
13. C. R. Van West, Ed., *Reconstructing Prehistoric Climatic Variability and Agricultural Production in Southwestern Colorado, A.D. 901–1300: A GIS Approach* (Mesa Verde Museum Association, Mesa Verde, CO, 1991).
14. T. L. Jones et al., *Curr. Anthropol.* **40**, 137 (1999).
15. R. B. Alley et al., *Nature* **362**, 527 (1993).
16. W. Dansgaard et al., *Nature* **364**, 218 (1993).
17. G. H. Denton, W. Karlen, *Quat. Res.* **3**, 155 (1973).
18. S. R. O'Brien et al., *Science* **270**, 1962 (1995).
19. G. Bond et al., *Science* **278**, 1257 (1997).
20. G. G. Bianchi, I. N. McCave, *Nature* **397**, 515 (1999).
21. P. deMenocal, J. Ortiz, T. Guilderson, M. Sarnthein, *Science* **288**, 2198 (2000).
22. L. D. Keigwin, *Science* **274**, 1503 (1996).
23. R. S. Bradley, P. D. Jones, *Climate Since A.D. 1500* (Routledge, London, 1995).
24. W. E. Dean, *Geology* **25**, 331 (1997).
25. L. D. Keigwin, R. S. Pickart, *Science* **286**, 520 (1999).
26. L. D. Keigwin, E. A. Boyle, *Proc. Natl. Acad. Sci. U.S.A.* **97**, 1343 (2000).
27. W. S. Broecker, S. Sutherland, T.-H. Peng, *Science* **286**, 1132 (1999).
28. G. S. Dwyer, T. M. Cronin, P. A. Baker, J. Rodriguez-Lazaro, *Geochim. Geophys. Geosyst.* **1**, 2000GC000046 (2000).
29. W. S. Broecker, G. Bond, M. Klas, G. Bonani, W. Wolfli, *Paleoceanography* **5**, 469 (1990).
30. T. J. Crowley, *Science* **289**, 270 (2000).
31. D. Rind, J. T. Overpeck, *Quat. Sci. Rev.* **12**, 357 (1993).
32. J. Beer, W. Mende, R. Stellmacher, *Quat. Sci. Rev.* **19**, 403 (2000).
33. J. Lean, J. Beer, R. Bradley, *Geophys. Res. Lett.* **22**, 3195 (1995).
34. E. R. Cook, D. M. Meko, C. W. Stockton, *J. Clim.* **10**, 1343 (1997).
35. W. Dean, T. S. Ahlbrandt, R. Y. Anderson, J. P. Bradbury, *Holocene* **6**, 145 (1996).
36. M. Stuiver, T. F. Braziunas, *Holocene* **3**, 289 (1993).
37. H. Weiss et al., *Science* **261**, 995 (1993).
38. J. N. Postgate, *Early Mesopotamia* (Routledge, New York, 1992).
39. H. Weiss, in *Engaging the Past to Understand the Future*, G. Bawden, R. Reyecraft, Eds. (Univ. of New Mexico Press, Albuquerque, 2000), pp. 75–98.
40. H. M. Cullen et al., *Geology* **28**, 379 (2000).
41. G. Lemcke, M. Sturm, in *Third Millennium B.C. Climate Change and Old World Collapse*, N. Dalfes, G. Kukla, H. Weiss, Eds., vol. 49 of *NATO ASI Series I* (Springer, Berlin, 1997), pp. 653–678.
42. M. Bar-Matthews, A. Ayalon, A. Kaufman, *Quat. Res.* **47**, 155 (1997).
43. H. M. Cullen, P. B. deMenocal, *Int. J. Climatol.* **20**, 853 (2000).
44. M. D. Coe, *The Maya* (Thames and Hudson, London, 1987).
45. J. W. G. Lowe, *The Dynamics of the Apocalypse* (Univ. of New Mexico Press, Albuquerque, 1985).
46. R. E. W. Adams, in *The Classic Maya Collapse*, T. P. Culbert, Ed. (Univ. of New Mexico Press, Albuquerque, 1973), pp. 21–34.
47. M. Brenner et al., in *Interhemispheric Climate Linkages* (Academic Press, New York, 2001), pp. 87–103.
48. R. B. Gill, *The Great Maya Droughts: Water, Life, and Death* (Univ. of New Mexico Press, Albuquerque, 2000).
49. D. A. Hodell, M. Brenner, J. H. Curtis, in *Imperfect Balance: Landscape Transformations in the Pre-Columbian Americas*, D. Lentz, Ed. (Columbia Univ. Press, New York, 2000), pp. 13–38.
50. D. A. Hodell, J. H. Curtis, M. Brenner, *Nature* **375**, 391 (1995).
51. J. H. Curtis, D. A. Hodell, M. Brenner, *Quat. Res.* **46**, 37 (1996).
52. I. Shimada, C. B. Schaaf, L. G. Thompson, E. Mosley-Thompson, *World Archaeol.* **22**, 247 (1991).
53. L. G. Thompson, M. E. Davis, E. Mosley-Thompson, *Hum. Ecol.* **22**, 83 (1994).
54. A. C. Paulsen, *World Archaeol.* **8**, 121 (1976).
55. A. L. Kolata, *Tiwanaku and Its Hinterland* (Smithsonian Institution Press, Washington, DC, 1996).
56. M. W. Binford et al., *Quat. Res.* **47**, 235 (1997).
57. H. Weiss, R. S. Bradley, *Science* **291**, 609 (2001).
58. E. Cook kindly provided the U.S. drought reconstruction maps shown in Fig. 1. This manuscript greatly benefited from discussions with E. Cook, D. Hodell, and M. Brenner. Critical reviews were provided by H. Weiss, O. Bar-Yosef, E. Cook, and two anonymous reviewers.

REVIEW

Range Shifts and Adaptive Responses to Quaternary Climate Change

Margaret B. Davis* and Ruth G. Shaw

Tree taxa shifted latitude or elevation range in response to changes in Quaternary climate. Because many modern trees display adaptive differentiation in relation to latitude or elevation, it is likely that ancient trees were also so differentiated, with environmental sensitivities of populations throughout the range evolving in conjunction with migrations. Rapid climate changes challenge this process by imposing stronger selection and by distancing populations from environments to which they are adapted. The unprecedented rates of climate changes anticipated to occur in the future, coupled with land use changes that impede gene flow, can be expected to disrupt the interplay of adaptation and migration, likely affecting productivity and threatening the persistence of many species.

Modern plant taxa have persisted through a long period of variable climate, including glacial-interglacial cycles with large changes in temperature, precipitation, and CO₂ concentration, over the past 2.5 million years. Rates of climate change varied widely: Regional temperature changes were as rapid as several degrees Celsius within a few decades or as slow as 1°C per millennium. The changes in species distribution evidenced by fossils provide a detailed record of plant responses to these changes. Hundreds of pollen diagrams, compiled in databases, provide re-

gional and continental records of tree abundances as they changed through space and time (1–3). New pollen records supplemented by macrofossils (4) and DNA recovered from fossil pollen (5) provide increasing temporal and taxonomic detail. In arid regions, where pollen-bearing sediments are less abundant, plant fragments preserved in middens made by packrats (*Neotoma*) and other rodents provide a spatially precise record of past species distributions (6). Changes in geographic distribution are so frequently documented in the fossil record that range shifts are seen as the expected plant response to future climate change (7).

Beyond changes in distribution, however, plants underwent genetic changes, adapting to changes in climate during the Quaternary.

Yet adaptation at the population level is seldom considered in the literature describing Quaternary environments nor, with some notable exceptions (8–10), in discussions of vegetation response to anticipated global change.

Here we cite evidence of genetic adaptation to climate and argue that the interplay of adaptation and migration has been central to biotic response to climate change. Moreover, we discuss how rapid climate change challenges this process, pushing populations to limits of adaptation, thus influencing regional ecosystem properties as well as the persistence of taxa.

Range Shifts During the Late Quaternary

Range shifts are the most conspicuous, and best documented, response of woody species to Quaternary climate. As the climate warmed at the end of the last glacial interval, tree populations became established at higher latitudes. These range extensions are called “migrations,” although individual plants, unlike animals, cannot move to follow changing climate. Rather, occupation of new regions occurs through passive seed dispersal and establishment of seedlings in sites where conditions permit. The patterns of migration dur-

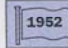
Department of Ecology, Evolution and Behavior, University of Minnesota, Saint Paul, MN 55108, USA.

*To whom correspondence should be addressed. E-mail: mbdavis@ecology.umn.edu

LEGENDA

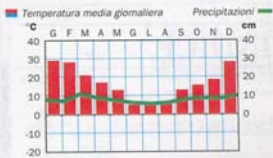
QUI VENGONO ILLUSTRATI TUTTI I GRAFICI, i simboli e gli indicatori di tendenza presenti nel testo.

PROFILO DELLA NAZIONE

 Data della dichiarazione d'indipendenza o della formazione della Nazione.

CLIMA

▷ Vengono indicati i tipi di clima che si registrano nelle diverse zone del Paese.





Qui vengono riportati i dati statistici, riferiti alla

capitale, delle massime estive e delle minime invernali.


TRASPORTI


▷ Viene indicato se nel Paese si tiene la guida a destra o a sinistra.

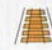
 Principale aeroporto internazionale del Paese con numero di passeggeri annuo.


 Tonnellaggio totale della flotta nazionale mercantile o da carico.

LA RETE DEI TRASPORTI
Infrastrutture nazionali di comunicazione (in km).

 Estensione della rete stradale asfaltata.


 Estensione della rete autostradale.

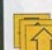
 Estensione della rete ferroviaria.

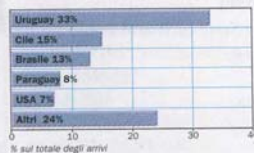
 Estensione della rete di canali navigabili a uso commerciale.

TURISMO


▷ Viene indicato il rapporto fra il numero di visitatori stranieri e la popolazione.

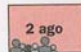
 Numero di visitatori all'anno, compresi i viaggiatori d'affari.

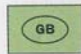
 Indicatore del trend recente del numero di visitatori all'anno (in aumento/stazionario/in calo).



Viene illustrata l'industria turistica o vengono indicati i motivi della sua assenza. Il grafico mostra la divisione in percentuale dei turisti per aree di provenienza.


 Data in cui sono stati stabiliti gli attuali confini.


 Festa nazionale.


 Sigla automobilistica.


POPOLAZIONE

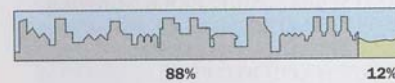
▷ Indicazione generale della densità di popolazione in ogni Paese (alta/media/bassa).

 Principali lingue parlate, in ordine decrescente di importanza.

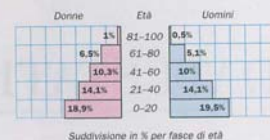
 Densità media della popolazione in tutto il Paese.

 Percentuale degli affiliati alle diverse confessioni fra quanti professano una religione.

 Percentuale delle diverse etnie presenti nel Paese.



Rapporto tra popolazione che abita in aree urbane (grigio) e rurali (verde).




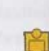
Suddivisione in % per fasce di età

In questo grafico si suddivide la popolazione per sesso e fasce d'età, fornendo così un interessante spaccato della demografia del Paese.

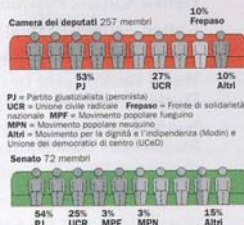
POLITICA

▷ Viene indicato se nel Paese si tengono elezioni multipartitiche democratiche.


 Date delle ultime e delle prossime elezioni politiche per la Camera alta (A.) e bassa (B.).

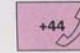
 Nome del capo di Stato. In molti casi questa è una carica onorifica e non corrisponde alla figura di maggior potere nel Paese.


Il grafico rappresenta la composizione politica del governo del Paese, basata sui risultati di ogni partito alle ultime elezioni. Laddove ci sono due Camere, la più importante viene illustrata al primo posto.



PJ = Partito giustiziarista (peronista)
UCR = Unione civile radicale
MPF = Movimento popolare fuerguano
MPN = Movimento popolare neuquino
Altri = Movimento per la dignità e l'indipendenza (Modin) e Unione dei democratici di centro (UCDC)


 Fusi orari (la differenza oraria è calcolata rispetto a Greenwich).


 Prefisso telefonico internazionale.

 Codice Internet di identificazione del Paese.

POLITICA ESTERA


▷ Viene indicato se il Paese fa parte dell'ONU, e l'eventuale data di ingresso.

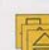
 Indicazione delle organizzazioni internazionali cui il Paese appartiene.

 Il Paese non appartiene ad altre organizzazioni internazionali.

CONTRIBUTI


▷ Viene indicato se il Paese dà (donatore) o riceve (beneficiario) contributi internazionali.


 L'ammontare dei contributi, dati o ricevuti, è espresso in Dollari. Non sono compresi i dati riservati sui finanziamenti militari.

 Vengono indicate le variazioni nell'ammontare dei contributi (in aumento/stazionario/in calo).

DIFESA


▷ Viene indicato se nel Paese c'è servizio militare obbligatorio.


 Il budget per la difesa: le spese statali annue (in Dollari) per armi e personale militare.


 Vengono indicate le variazioni del trend delle spese per la Difesa (in aumento/stazionario/in calo).

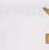
LE FORZE ARMATE

I simboli rappresentano i principali settori delle Forze armate nazionali.

 Esercito: dotazioni e personale.


 Marina: dotazioni e personale.

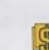
 Aeronautica: dotazioni e personale.

 Armi nucleari.

ECONOMIA

▷ Si dà un'indicazione dell'inflazione media registrata nel corso dell'ultimo decennio.

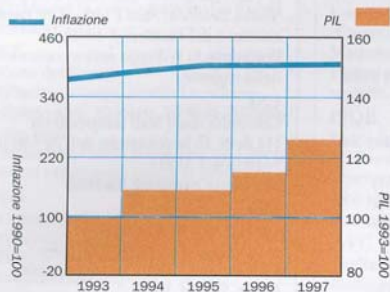
 Prodotto nazionale lordo (PNL), il valore complessivo di beni e servizi prodotti da una Nazione.

 Variazione del cambio della valuta locale con il Dollaro nel corso dell'ultimo anno.

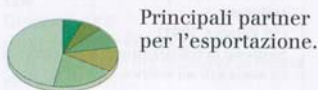
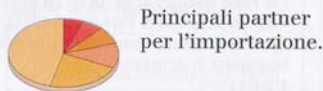
PNL: POSIZIONE IN CLASSIFICA MONDIALE.....24*
PNL PRO CAPITE.....\$24.388
BILANCIA DEI PAGAMENTI.....\$2.2mld
INFLAZIONE.....5,6%
DISOCCUPAZIONE.....10,6%

Con questi dati si vuole fornire un quadro generale

dell'economia della Nazione. Il PNL, diversamente dal PIL, comprende le entrate da investimenti e attività svolte all'estero. La bilancia dei pagamenti è data dalla differenza tra le entrate e le uscite con l'estero.



Questo grafico mostra, anno per anno, le variazioni del PIL e dei prezzi al consumo.



RISORSE

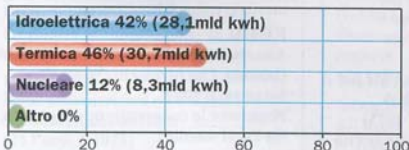
Viene indicata la produzione energetica nazionale complessiva (in kw).

Petrolio, in barili al giorno (b/g). Si indicano anche le attività di raffinazione, le riserve di petrolio e di altri combustibili fossili.

Numero stimato dei capi di bestiame.

Principali riserve minerali, in ordine decrescente di importanza economica.

Pescato annuo (nei Paesi in cui la pesca è una voce economica importante).



Suddivisione in % per fonte energetica

Rappresentazione grafica dell'uso delle diverse fonti energetiche per la produzione di elettricità (al secondo punto si allude alla combustione di legno, combustibili fossili ecc.). Nel testo viene presentato un quadro generale delle risorse naturali del Paese.

AMBIENTE

Viene indicato se i Verdi fanno parte del governo nazionale.

Percentuale del territorio protetto per legge. La protezione è spesso solo teorica.

Indice di consumo ambientale - basato su un rapporto del WWF (in aumento/stazionario/in calo).

TRATTATI AMBIENTALI INTERNAZIONALI
Viene indicato se il Paese ha sottoscritto i seguenti trattati ambientali.

Ramsar: protezione aree umide. Protocollo di Montreal: emissioni di CFC.

CITES: specie a rischio di estinzione. CBD: biodiversità.

Basilea: rifiuti tossici. Kyoto: effetto serra.

MEDIA

Viene indicato il tasso di diffusione di televisori nel Paese.

Nessuna o lieve censura politica sui media nazionali.

Parziale censura politica sui media nazionali.

Totale censura politica sui media nazionali.

MEDIA CARTACEE ED ELETTRONICHE
Stampa ed emittenti nazionali (dimensioni e proprietà).

Principali quotidiani nazionali.

Televisioni: pubbliche/private.

Radio: pubbliche/private.

CRIMINALITÀ

Viene indicato se nel Paese è usata la pena di morte.

Popolazione carceraria.

Trend generale della criminalità (in aumento/stazionario/in calo).



Qui vengono riportati solo i dati ufficiali sulla criminalità.

CRONOLOGIA

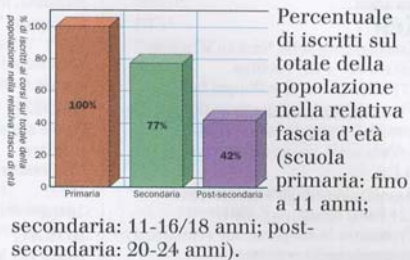
Partendo da una data significativa nella storia recente della Nazione, la cronologia sintetica prosegue fino a oggi e illustra i momenti fondamentali e i punti di svolta.

ISTRUZIONE

Viene indicata la durata dell'obbligo scolastico.

Tasso di alfabetizzazione. Per l'UNESCO è alfabetista chi sa leggere e scrivere un breve testo.

Numero di studenti universitari (% valutata sulla popolazione tra i 20 e i 24 anni).



SANITÀ

Viene indicato se c'è una forma di servizio sanitario pubblico.

Rapporto tra il numero dei medici e la popolazione.

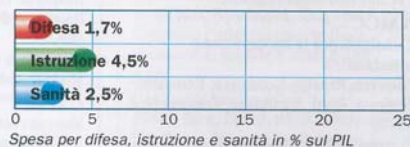
Elenco delle principali cause di morte.

SPESE

Viene indicato il trend del PIL pro capite nel corso dello scorso decennio (in aumento/stazionario/in calo).

Numero di automobili possedute ogni 1000 abitanti.

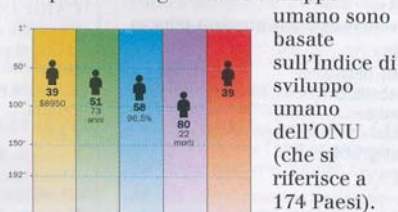
Numero di linee telefoniche ogni 1000 abitanti.



Percentuale del PIL spesa per difesa, istruzione e sanità.

POSIZIONE NEL MONDO

Le classifiche per scolarizzazione, compimento degli studi e sviluppo



PIL pro capite in \$
Aspettativa di vita
Alfabetizzazione
Mortalità infantile (ogni 1000 nati vivi)
Indice di sviluppo umano